

RAL 93096

COPY 1 R61 RR

Acc: 221609

RAL-93-096 Science and Engineering Research Council

Rutherford Appleton Laboratory

Chilton DIDCOT Oxon OX11 0QX

RAL-93-096

AP, INST

The Experimental Characterisation of Gas Microstrip Detectors: II. Counting Rate Characteristics

J E Bateman and J F Connolly

December 1993

Science and Engineering Research Council

"The Science and Engineering Research Council does not accept any responsibility for loss or damage arising from the use of information contained in any of its reports or in any communication about its tests or investigations"

THE EXPERIMENTAL CHARACTERISATION OF GAS MICROSTRIP DETECTORS

II. COUNTING RATE CHARACTERISTICS

J E Bateman and J F Connolly
Rutherford Appleton Laboratory, Chilton, Didcot, OX11 0QX, U.K.

The results of a programme of research into the experimental properties of gas microstrip detectors are reported. In this report information on the counting rate characteristics of the devices is presented.

1. INTRODUCTION

Since its introduction by Oed [1], the gas microstrip detector (GMSD) has been studied by several groups for potential applications in high energy physics, space science, materials science and medicine.[2-8] The GMSD is a form of the gas proportional counter in which an extremely precise pattern of metallisation is laid down on an insulating substrate using standard microlithographic techniques. The pattern consists of interleaved narrow (typically $10\mu\text{m}$) and wide (typically $100\mu\text{m}$) metal strips separated by (typically) around $100\mu\text{m}$ strips of insulating substrate. Application of a few hundred volts between the anode and cathode strips in a suitable gas atmosphere results in amplification factors of up to 10000 for any free electrons captured by the anode. Figure 1 shows a typical detector structure with a drift electrode spaced a few millimeters away from the lithographic plate to define the active volume of the detector.

As a potential replacement for the multiwire proportional counter (MWPC) the GMSD has several attractions. First, independent detectors can be made on a pitch of 0.25mm or less; second, the positional accuracy of the electrodes essential for all gas detectors can be achieved easily and without the demand for structural strength which wire tensions impose on the MWPC; third, the very small anode-cathode gap leads to sub-microsecond positive ion transit times thus permitting count rate densities two orders of magnitude higher than is possible with a wire counter. The excellent spatial resolution ($< 30\mu\text{m}$) has been demonstrated in high energy particle tracking [3] and the structural precision has permitted excellent energy resolution [5].

The undoubted potential of the GMSD was vitiated throughout its early development by the presence of gain instabilities which are severely aggravated by high counting rates so robbing it of its one great advantage over a wire counter. This gain instability was quickly determined to be a result of the effect of the very high electric fields at the edge of the anode on the substrate material. In extensive tests with conventional glasses (pyrex, etc) [9] the well-known ionic polarisation effects of such materials were shown to be responsible. When it was suggested [10,11] that semiconducting glasses might offer a more stable substrate we immediately obtained samples and produced GMSDs on them. The resulting detectors showed a degree of stability and reproducibility which, for the first time, made systematic measurements on our GMSDs possible.

The following results and analysis show the limits set to the counting rate capabilities of the GMSD by the positive ion transit times in the detector, once the substrate-induced effects have been overcome. As with all gas counters, the positive ion transit effects set an upper limit to the rate performance of the devices, and this limit will be shown to be rather more restrictive than one might expect.

Test detectors were fabricated using the basic pattern of figure 1. In the lithography 20 anodes (60mm long) are bussed together with a connecting pad at the outboard end and the corresponding cathodes are similarly treated. This results in an active detector area of 6mm x 60mm with this pattern repeated five times on a standard 100mm x 100mm glass plate giving five independent detectors. The metalisation was generally aluminium and two distinct types of semiconducting glass were used - Schott S8900 ($10^{11} \Omega\text{-cm}$) and Pestov P9 ($10^9 \Omega\text{-cm}$) [10]. Some of the processing was carried out by VTT in Finland and some (using a gold metalisation) was arranged by Yu N Pestov at the BINR at Novosibirsk.

In order to be able to make use of smaller glass samples, a test pattern was designed which restricted the length of the active detector area to 15mm and so accommodated the structures within an area of 50mm x 50mm.

The gas mixtures used were either argon+20% methane (premixed) or argon+25% isobutane, flowed through the detector box. X-ray stimulation was derived from a Cu-anode X-ray generator.

2. PULSE FORMATION AND GAIN CHARACTERISTICS

The operating potentials used in our tests were generally $V_a=0V$, $V_c=-600V$ to $-800V$ and $V_d=V_c$ to $-3000V$ (figure 1). These potentials result in an electric field configuration in the gas above the plate of the form illustrated in figure 2. (This shows the field lines in a plane transverse to the strip pattern on the plate.) The characteristic of this pattern is that the field configuration divides into two clearly defined regions, a dipole region within one pattern pitch of the plate and a drift region with an approximately uniform electric field filling the rest of the conversion space. When $V_d=V_c$, the mean attractive potential for electrons of our metal strip pattern can be estimated as $\approx V_c/3$ (assuming the potential across the plate is graded by the conducting substrate) so giving an effective electron drift field of $(V_d - 2V_c/3)/d$, where d is the separation of the drift electrode and the plate. A standard test configuration for gain tests is to set $V_d=V_c$, so giving a collecting field of $V_c/3d$.

2.1 Positive Ion Motion

In GMSPDs, (as is well known for wire counters [12]), both pulse shape and counting rate effects are governed almost exclusively by the movement of the positive ion cloud generated by the avalanche. As noted above, the electric field (figure 2) which transports the positive ions divides into two distinct regions, the dipole field close to the plate surface and the uniform field in the conversion gap of the GMSPD. In the dipole region, the mean electric field experienced by the ions is of the order of $2V_c/p$, where p is the pitch of the anode-cathode pattern on the plate. Assuming a positive ion mobility (μ) of $2(\text{cm/s})/(\text{V/cm})$ and $V_c=-700V$ this leads to an ion collection time (T_c) of $\approx 0.16\mu\text{s}$. On the other hand, any ions taking the route to the drift electrode experience a much lower electric field $(V_d - V_c)/d$ over the much greater distance d (9mm in our case). Assuming $V_d=-2000V$, the ion transit time for this component is $T_d=290\mu\text{s}$. Figure 3 shows the signal charge induced on the anode when the charge divides between the two paths.

The three orders of magnitude ratio between T_d and T_c simplifies the analysis and allows us to say that (i) the charge captured in a fast pulse ($< 1\mu\text{s}$ decay time) shaper is determined solely by the fraction of the charge that is collected in the dipole field and (ii) the rate limitation of the GMSPD will be determined chiefly by the ion drift in the uniform-field region.

That rate effects caused by the positive ion movement in the dipole field region are negligible can be shown by using the calculations of Hendricks [13] for rate effects in a cylindrical proportional counter. Inserting the dimensions of the anode strip and the anode-cathode along with the ion transit time of $0.16\mu\text{s}$ into the Hendricks formula gives an order of magnitude

estimate that the most extreme operating conditions imaginable for a GMSD (say, a flux of $1\text{MHz}/\text{mm}^2$ of 8keV x-rays at a gas gain of 10^4) will result in an anode potential shift of mV magnitude with negligible effect on the gas gain.

Employing their numerical solution for the electric field in a typical GMSD (the most significant difference from the configuration of figure 1 is that the drift region of their model is 4mm compared with 9mm in our case) Florent et al [14] were able to estimate the division of the ion charge between the two cathodes. They showed that with $V_d = V_c$ 3.5% of the avalanche signal flowed to the drift cathode, this fraction rising to 70% at $V_d = -3000\text{V}$. For most of the working range of V_d the fraction (f) rises approximately linearly with the fit $f = 0.035 + 2.6 \cdot 10^{-4} V_d$. Since the division of charge between the two field zones can only depend on the relative strengths of the fields in the region above the anode, we can scale this slope term in this formula to take account of the lower field in our GMSD design by simply multiplying by $4/9$ (the ratio of the drift space widths) to get an approximate relation for f :

$$f = 0.035 + 1.15 \cdot 10^{-4} V_d. \quad (1)$$

2.2 The Gain Contribution of the Drift Potential

Figure 4 shows the dependence of the gain of a GMSD as a function of the potential on the drift electrode. In the figure the gain is normalised to the gain in the standard configuration of $V_d = V_c$. We observe that V_d and V_c make approximately independent gain controls with the contribution from V_d being very weak at around 25% increase in gain for every 1000V increase in V_d . This is not surprising in view of the fact that the drift electrode is 90 times further away from an anode than the adjacent cathode. However, the linear dependence of the gain on V_d is surprising: one would expect an exponential type dependence (however weak).

This linear gain curve can be understood in terms of the charge sharing discussed above: increasing V_d increases the total avalanche gain but, at the same time, increases the fraction of the signal going to the drift cathode and so reduces the fast part of the signal seen in the amplifier (figure 3). Dividing the observed gain vs V_d curve by $(1-f)$ (as defined in (1) above) provides the "true" gas gain contribution from V_d . As figure 5 shows this is indeed an exponential type function as the fit shows.

3. COUNTING RATE CHARACTERISTICS

The factor of $10^2 - 10^3$ difference in the positive ion transit times between the two sections of the electric field leads one to believe that, until counting rate fluxes become very high ($\approx \text{Mhz}/\text{mm}^2$), the rate effects observed in the GMSD will be dominated by the build up in the drift region of space charge which will screen the plate from the drift cathode and so reduce the gain as the flux increases. The very slow transit time (hundreds of μs) is compensated for by the weak effect that V_d has on the gas gain.

3.1 Space Charge in a Parallel Gap

The space charge in the drift section of a GMDS can be modelled as a planar source of current distributed over the plate surface being transported by a uniform electric field. The current density is:

$$j = RP \quad (2)$$

where we have a rate of R per unit area of detector per second of avalanches of pulse height P coulombs. Also, by definition:

$$j = \sigma v = \sigma \mu V/d \quad (3)$$

where σ is the charge density, v is the ion drift velocity, μ is the ion mobility, V is the effective potential (see above) across the drift gap of width d .

Rearranging (2) and (3) one finds that:

$$\sigma = RPd/\mu V \quad (4)$$

In equilibrium a parallelepiped of unit area across the drift gap contains a total amount of charge:

$$\sigma \times 1 \times 1 \times d = RPT$$

where T is the positive ion drift time across the gap. It follows that:

$$T = d^2/\mu V$$

In order to evaluate the potential developed by the space charge we must integrate Poissons equation with the appropriate boundary conditions:

$$d^2V/dx^2 = \sigma/\epsilon_0$$

The solution is:

$$-\delta V = \sigma d^2/2\epsilon_0$$

which is (substituting for σ)

$$-\delta V = RPd^3/2\epsilon_0\mu V \quad (5)$$

Equation (5) is interpreted as defining the effective reduction in the mean local potential difference between the plate and the drift electrode caused by the presence of the space charge density σ in the drift gap.

Only the positive ions which travel to the drift cathode can contribute to the space charge so we must incorporate the fraction "f" defined in (1) above in (5). Further, the pulse height measured experimentally (Q) is that charge in the fast part of the pulse: $Q = (1-f)P$. Thus:

$$-\delta V = fRQd^3/2\epsilon_0\mu V(1-f) \quad (6)$$

Using the data already to hand (equation (1) and the gain fit from figure 4) we can evaluate $-\delta V$ for some typical working conditions in a GMSD. Figure 6 shows the dependence of $-\delta V$ on V_d when a GMSD is run at a gain of 561 and a flux of 55kHz/mm². As V_d increases $-\delta V$ declines to a shallow minimum at about 700V effective potential before rising slowly again. The maximum excursion in $-\delta V$ is $\approx 7V$, which, figure 4 tells us, will result in an increase in gain of 0.18%. Figure 6 tells us that, to first order, the rate performance of a GMSD is independent of the drift potential. This is confirmed in practice and means that the drift field may be selected to suit the criteria of maximum gain and fast electron collection.

3.2 Experimental Measurements

All our early GMSDs were fabricated on conventional (i.e. semi-insulating) glasses. As noted elsewhere [9] gain instability on such substrates made systematic measurements difficult. In addition to gain instability following the application of bias, a rate dependent instability was also observed. Figure 4 shows the behaviour of the gain (initially ≈ 850) of one of our standard test counters fabricated on Tempax (a borosilicate glass) when various rates of x-rays were applied to an area of 1mm². (In each case the beam was moved to a fresh spot on the counter for the measurement.) The data of figure 7 shows that, not only is the depression of gain with rate much larger (by an order of magnitude) than the deficit estimated for the space charge effects but that a response time constant of minutes is observed. This can clearly have no relation to gaseous space charge effects which have a maximum time constant of the order of a millisecond. Substrate polarisation does have time constants of the order of minutes and is clearly the cause of the severe rate effects observed in figure 7. Recovery of the gain in the locality of the x-ray beam after its removal takes ≈ 60 minutes after an irradiation period of only 15 minutes at a flux of $\approx 20\text{kHz/mm}^2$ (figure 8). The severe and highly localised response of the gain to any significant signal flux and the long time constants involved make it unlikely that substrates of this type will provide GMSDs for any practical applications.

Fabricating GMSDs on substrates of semiconducting glass results in a dramatic improvement in both the stability and the rate performance of the devices. On applying bias, a small (-5%) gain shift is observed which stabilises in ≈ 30 seconds and when high x-ray fluxes are applied and removed, the gain returns intantaneously to its previous low-rate vale. It would appear therefore that it may be meaningful to interpret the gain versus rate dependence of devices made on semiconducting glass in terms of the model discussed above.

Figure 9 shows the gain versus rate curve for a test counter fabricated on P9 glass. The x-ray beam is irradiating approximately 1mm^2 of counter. The fit formula is simply the gain formula derived from figure 4 with V_d modified by the space charge term. Thus the measured gas gain (G) is:

$$G = G_0(1 - 2.5 \cdot 10^{-4} \cdot \delta V)$$

where δV is calculated from equation (6) and G_0 is the gas gain at low rates (1168). The fraction of charge going to the drift cathode is left as the single free parameter in a fit to the data. (The measured gain represents only that fraction of the pulse height collected by the plate cathodes due to the fact that our amplifier time constant (bipolar delay line) is $1\mu\text{s}$.) The fit of figure 9 indicates that $f = 0.34$ while equation (1) predicts $f = 0.32$. Given the approximations made, we feel that this result is satisfactory and confirms that GMSDs fabricated on semiconducting glasses perform (as far as rate is concerned) up to the natural limits set by positive ion motion in the gas.

In order to investigate the rate effects as a function of the drift potential we measured the ratio of the gas gain at $55\text{kHz}/\text{mm}^2$ to that at $2\text{kHz}/\text{mm}^2$ as a function of V (the effective drift potential). Figure 10 shows the results and compares them with the response calculated from the space charge model. Within the experimental error of $\pm 0.25\%$ the data supports the conclusion of the model that the rate performance is essentially independent of V .

4. CONCLUSIONS

GMSDs fabricated on conventional (semi-insulating) glass substrates show severe and unstable changes in gain as a function of the event flux on the plate. A model of the space charge effects caused by positive ion movements in the drift space of the counter shows that such effects are an order of magnitude too large and show time constants typical of substrate polarisation rather than positive ion movements in the gas. On the other hand, GMSDs fabricated on semiconducting glass substrates show stable gain characteristics and rate effects which agree quite accurately with the predictions of the space charge model.

The space charge model is simplified to consideration of the positive ion movement in the parallel-gap drift space of the GMSD by the three orders of magnitude difference in the positive ion transit times in the drift space and the dipole field region near the plate. Variation in the sharing of the charge between the two regions results in the linearising of the dependence of the effective gas gain (i.e. within $1\mu\text{s}$) on the drift field and the virtual independence of the rate effects on the value of the drift potential. (In general this means that one will elect to have as high a drift potential as possible in order to maximise the gain and minimise the electron collection time.)

In our standard GMSD, the rate effects are small but not negligible being (figure 9) of the order of a 6% gain loss at $250\text{kHz}/\text{mm}^2$ with pulses of 3.1×10^5 electrons. Looking at equation (6) for

δV we see that the critical design parameter is "d" the depth of the drift space since it appears as d^3 . Since f also depends on the field strength in the drift region we must consider the term $fd^3/(1-f)$. The behaviour of f as d varies is approximately such as to cancel out one d and leave δV increasing as d^2 (see equation(1) above).

In high energy physics applications it is desirable to keep the electron drift times as short as possible and drift gap widths of 3mm are employed [15] which reduces the rate effects by a factor of ten relative to those observed in figure 9. Such rate performance would appear to meet any possible application in this field.

In x-ray detectors for high rate imaging at synchrotron radiation facilities [6], a deeper detector drift region is generally called for in order to achieve a useful detection efficiency. In this case it is probably necessary to consider the space charge effect carefully in choosing the conversion depth. Increasing the gas pressure may prove useful since the ion mobility (μ) declines linearly with pressure while $\delta V \approx d^2/\mu$.

ACKNOWLEDGEMENTS

We are particularly indebted to Yu N Pestov of the Budker Institute of Nuclear Research, Novosibirsk for supplying us with the samples of P9 glass and a detector fabricated on this glass. We are grateful to Ilkka Suni and his colleagues at the Technical Research Centre of Finland (VTT) for their enthusiastic collaboration in the production of our GMSD plates. We would like to thank our colleagues Bernard O'Hagen, Adrian Walker and Aubrey Dobbs for their contributions to this work. Our thanks are also due to the staff of the RAL Central Microstructure Facility.

REFERENCES

1. A Oed, Nucl Instr & Meth A263 (1988) 351-359
2. F Angelini, R Bellazzini, A Brez, M M Massai, G Spandre and M R Torquati, Nucl Instr & Meth A283 (1989) 755-761
3. F Angelini, R Bellazzini, A Brez, M M Massai, G Spandre, M R Torquati, R Bouclier, J Gauden and F Sauli, IEEE Trans Nuc Sci 37 (no.2) 1990 112
4. F Hartjes, B Hendriksen and F Udo, Nucl Instr & Meth A289 (1990) 384
5. C Butz-Jorgensen, Rev Sci Instrum 63 (1) 1992 648
6. J E Bateman, J F Connolly, R Stephenson and J Morse, Proceedings of the European Workshop on X-ray Detectors for Synchrotron Radiation Sources, Aussois, France 1991

7. R Bouclier, J J Florent, J Gauden, A Pasta, L Ropelewski, F Sauli and L I Shekhtman, High flux operation of microstrip gas chambers on glass and plastic supports, presented at the Sixth International Wire Chamber Conference, Vienna, 1992, to be published in Nucl Instr & Meth
8. L I Shekhtman, High pressure gas avalanche chambers for medical radiology, presented at the Fourth International Conference on Application of Physics in Medicine and Biology, Trieste, 1992
9. J E Bateman and J F Connolly, Substrate-induced instability in gas microstrip detectors. RAL-92-085
10. G D Minakov, Yu N Pestov, V S Prokopenko and L I Shekhtman, Nucl Instr & Meth A326 (1993) 566-569
11. R Bouclier, G Million, L Ropelewski, F Sauli, Yu N Pestov and L I Shekhtman, Nucl Instr & Meth A332 (1993) 100-106
12. F Sauli, Principles of operation of multiwire and drift chambers, CERN 77-09
13. R W Hendricks, Rev Sci Instr 40 (1969) 1216
14. J J Florent, J Gaudaen, L Ropelewski and F Sauli, Nucl Instr & Meth A329 (1993) 125
15. J E Bateman, J F Connolly, R Stephenson, M Edwards and J C Thomson, The development of gas microstrip detectors for high energy physics applications, 3rd London Conference on Position sensitive Detectors, Brunel University, London, September 1993, (to be published in Nucl Instr & Meth)

FIGURE CAPTIONS

Figure 1

A schematic section of the gas microstrip detector used throughout the studies reported in this paper.

Figure 2

A schematic representation of the electric field pattern in a gas microstrip detector showing the two distinct regions: the (low) parallel collection field filling most of the space between the drift electrode and the plate and the region of intense field in the vicinity of the anode (adapted from field plots given in reference [2]).

Figure 3

This shows shows a schematic representation of the induced charge on the GMSD plate as a function of time in our detector assuming 30% of the positive ions (assumed to be CH_4 ions) flow to the drift cathode.

Figure 4

The gas gain relative to the condition $V_d = V_c$ is plotted as a function of $-(V_d - V_c)$ with various values of V_c for a GMSD fabricated on S8900 glass and operating in argon + 20% methane. The slopes of the straight line fits vary between 2.39%/100V and 2.6%/100V.

Figure 5

This shows the total gas gain of a GMSD as a function of the drift electrode potential ($V_d - V_c$) obtained by correcting the measured gas gain for the variable fraction of charge $(1-f)$ detected in the amplifier circuit. The linear curve of figure 4 becomes a gentle exponential curve in keeping with one's expectations of the avalanche gain mechanism.

Figure 6

This shows the evaluation of the space-charge-induced potential deficit on the drift gap ($-\delta V$) from the model (equation(6)) as a function of the effective drift potential ($V_d - 2V_c/3$) for a GMSD operating at a gain of 561 and a rate of 55kHz/mm² (the mobility value of methane ions is used). Over the practical range of V , $-\delta V$ changes by a maximum of 7V which leads to a very small change in the gain (< 1%).

Figure 7

The gain settling curves of a chrome/Tempax plate when the GMSD is required to deliver an increasing rate of x-ray-induced pulses. The beam spot is 1mm diameter. The pulse height is normalised to the initial value of 2.3×10^5 electrons. The x-ray beam was moved onto a fresh area of the plate for each measurement.

Figure 8

The short term recovery of the the GMSD gain (pulse height) after removal of a rate of 22.6kHz applied for ~20 minutes during the final measurement of figure 7.

Figure 9

The behaviour of the gas gain of a GMSD fabricated in gold on P9 glass when subjected to increasing event fluxes (8 keV x-rays). The fraction of positive ions going to the drift cathode is left as the only free parameter in the fit to the space charge model. The value of 34.2% accords well with that predicted by equation (1). Different detectors (on semiconducting glass) and different gain setting all give a similar level of agreement to the model as regards the general trend, but with different (but slight) systematic variations around the fit.

Figure 10

An experimental test of the independence of the rate-induced gain deficit as a function of the effective drift potential ($V = V_d - 2V_c/3$). The ratio of the gain at 2kHz/mm² to that at 55kHz/mm² is plotted as a function of V (gas gain = 561) with the prediction of the space charge model shown for comparison. The measurement errors are $\approx \pm 0.25\%$.

FIGURE 1

Drift Electrode (Vd)

9 mm

Cathode (Vc) Anode (Va)

150 μm

90 μm

10 μm



Back Plane (Vb)

1 mm

FIGURE 2

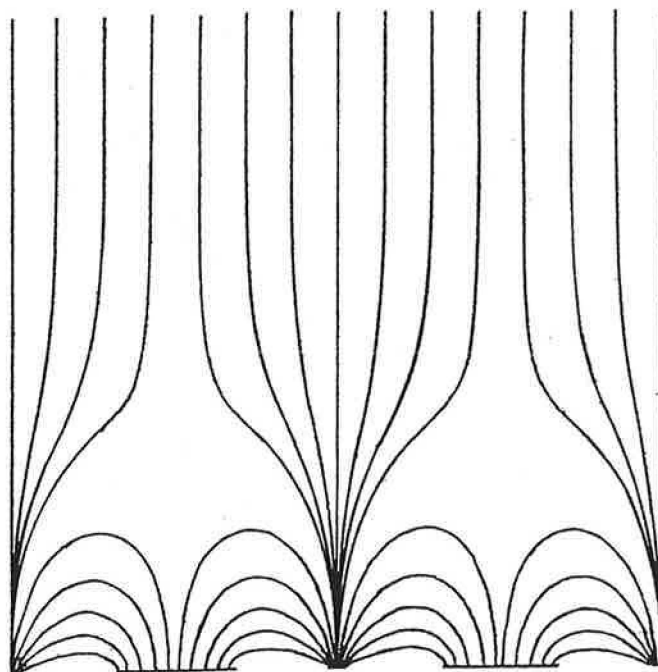


FIGURE 3

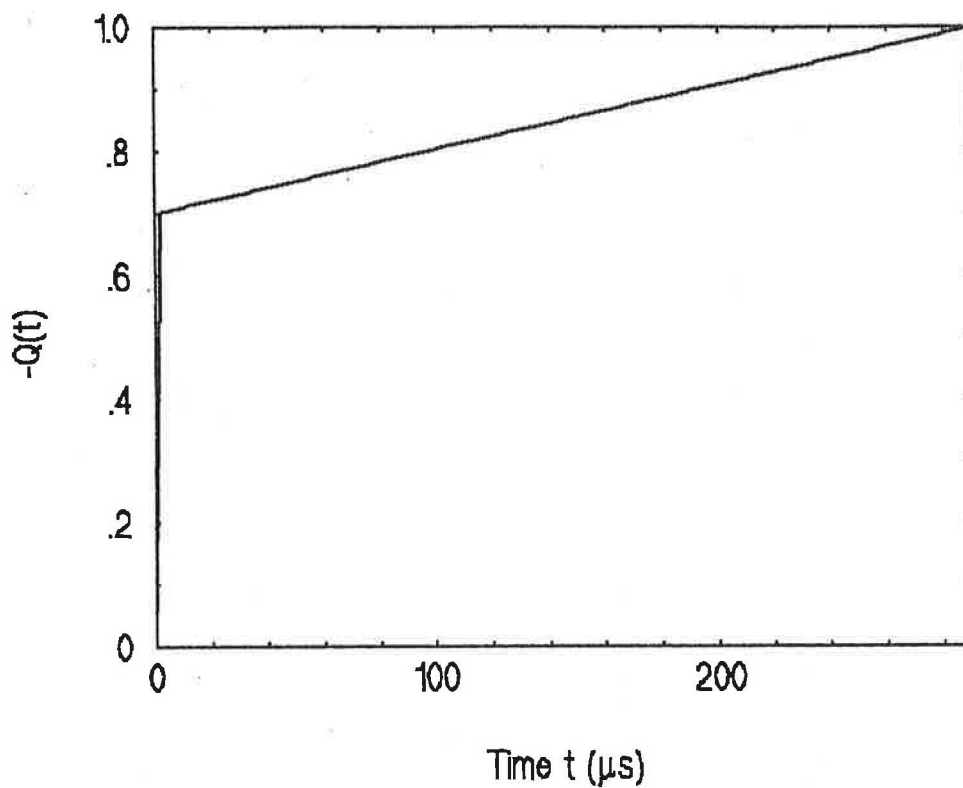


FIGURE 4

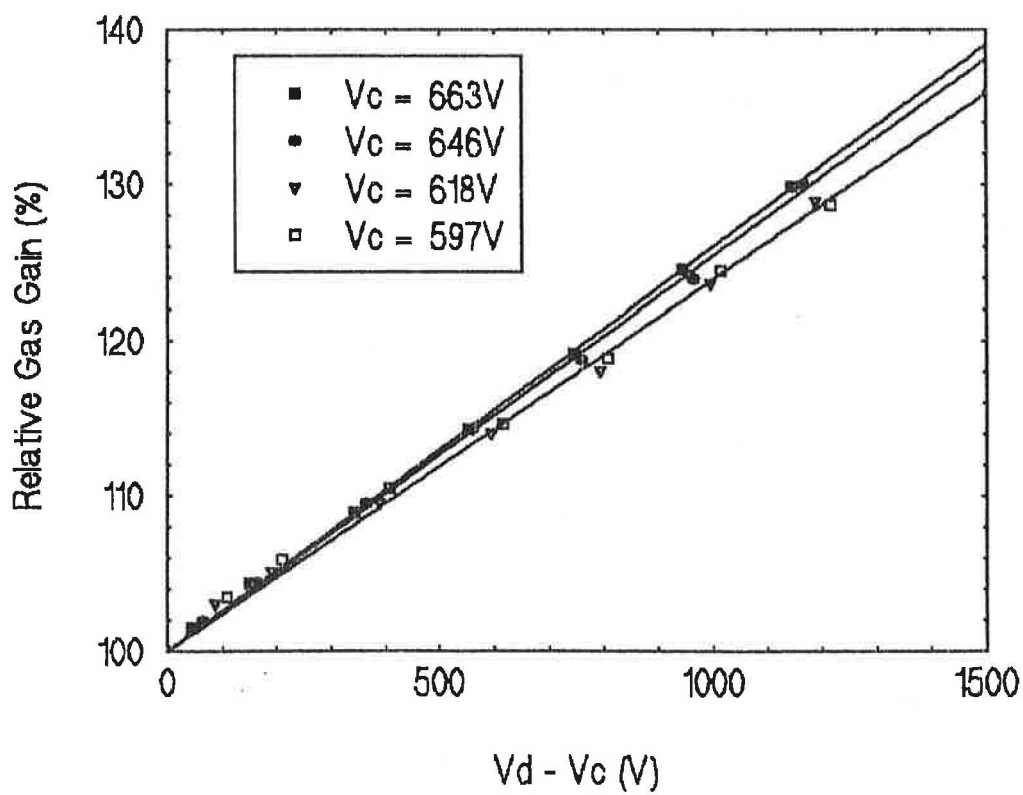


FIGURE 5

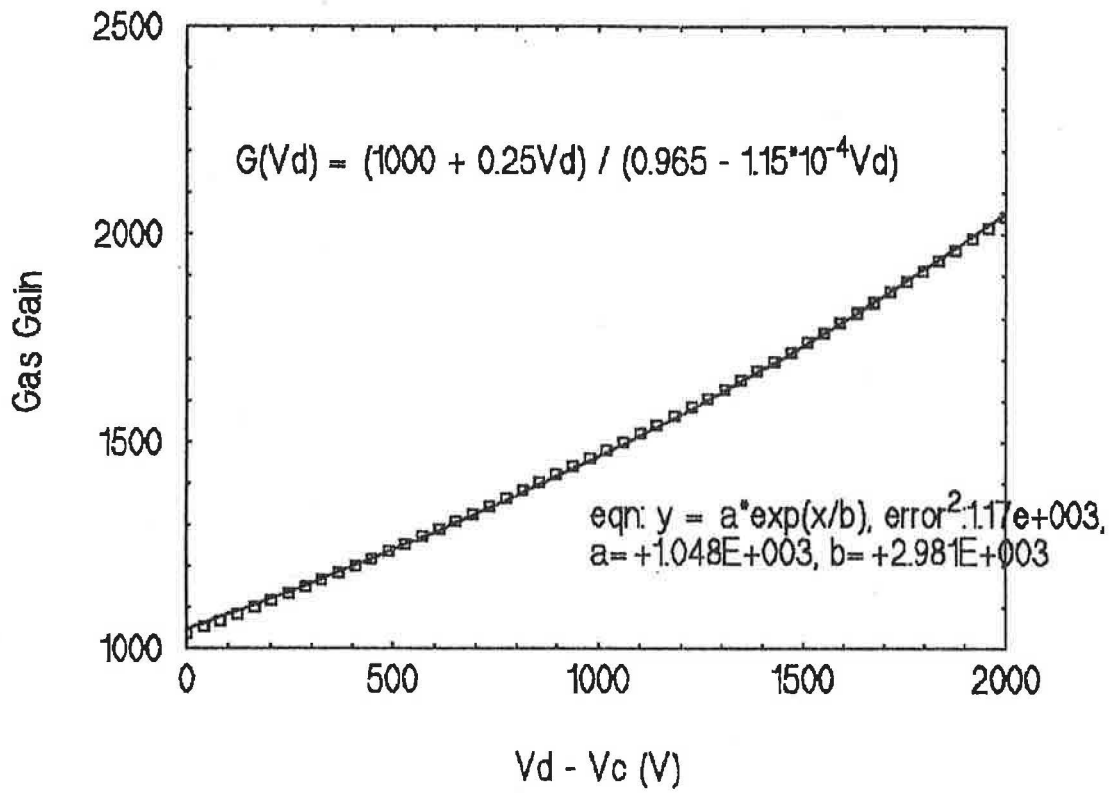


FIGURE 6

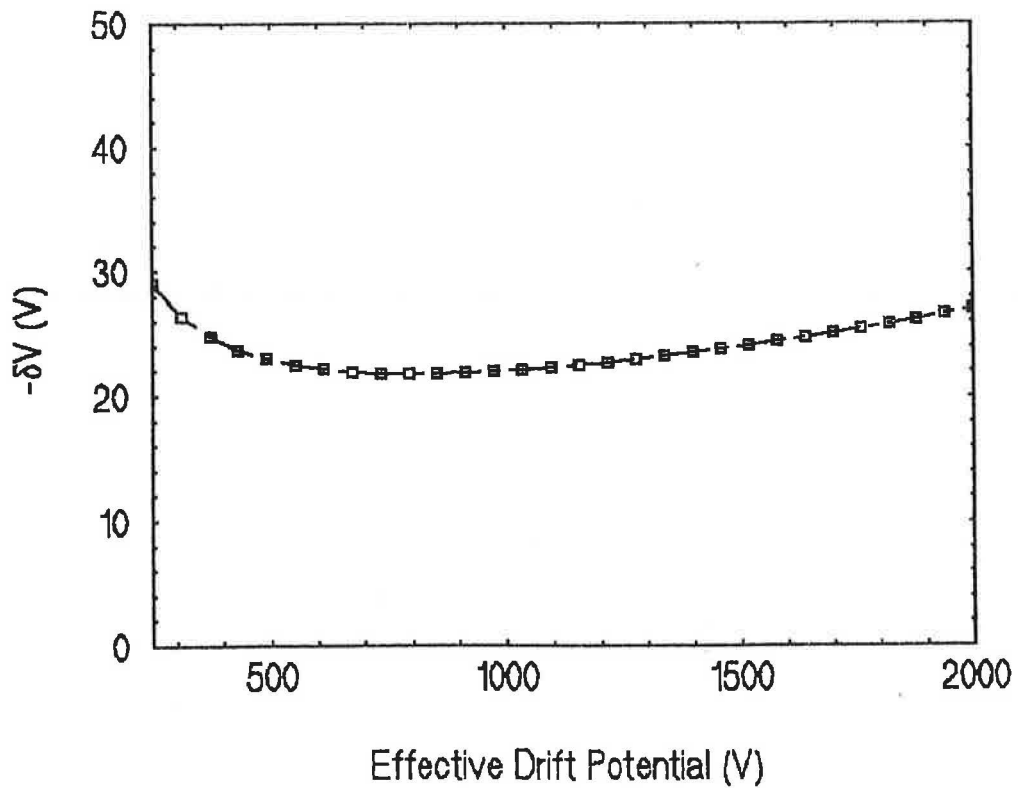


FIGURE 7

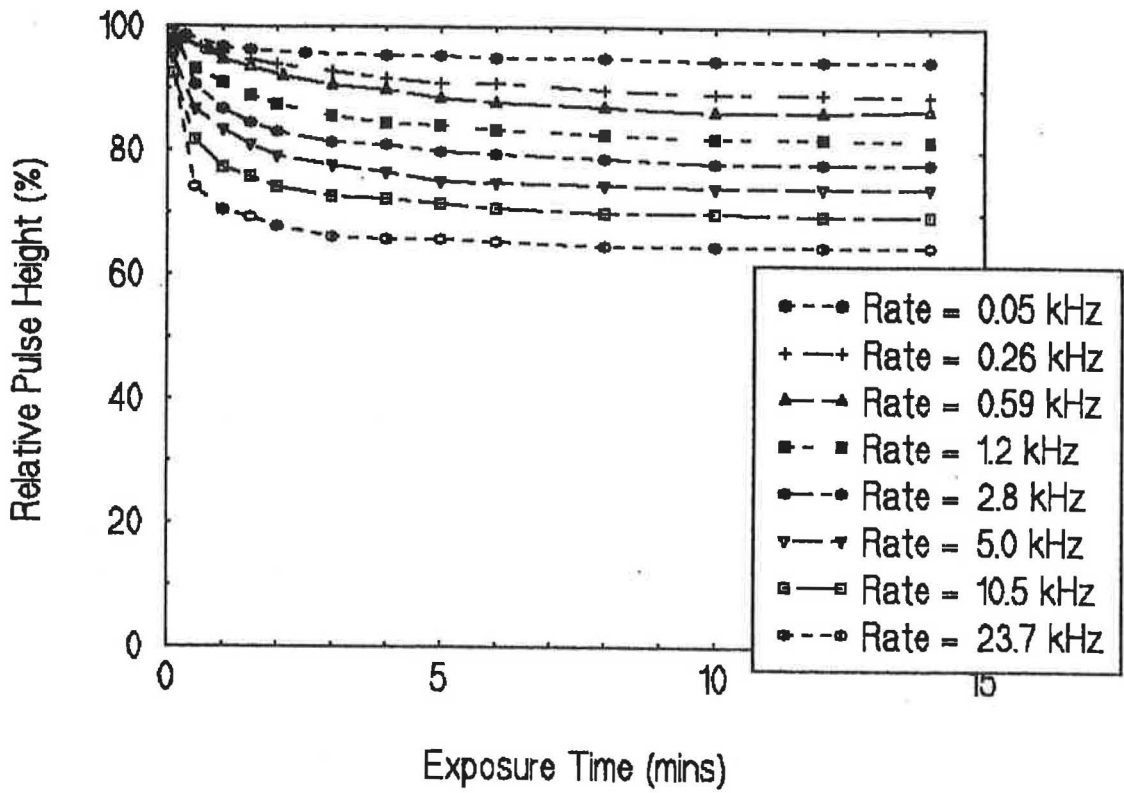


FIGURE 8

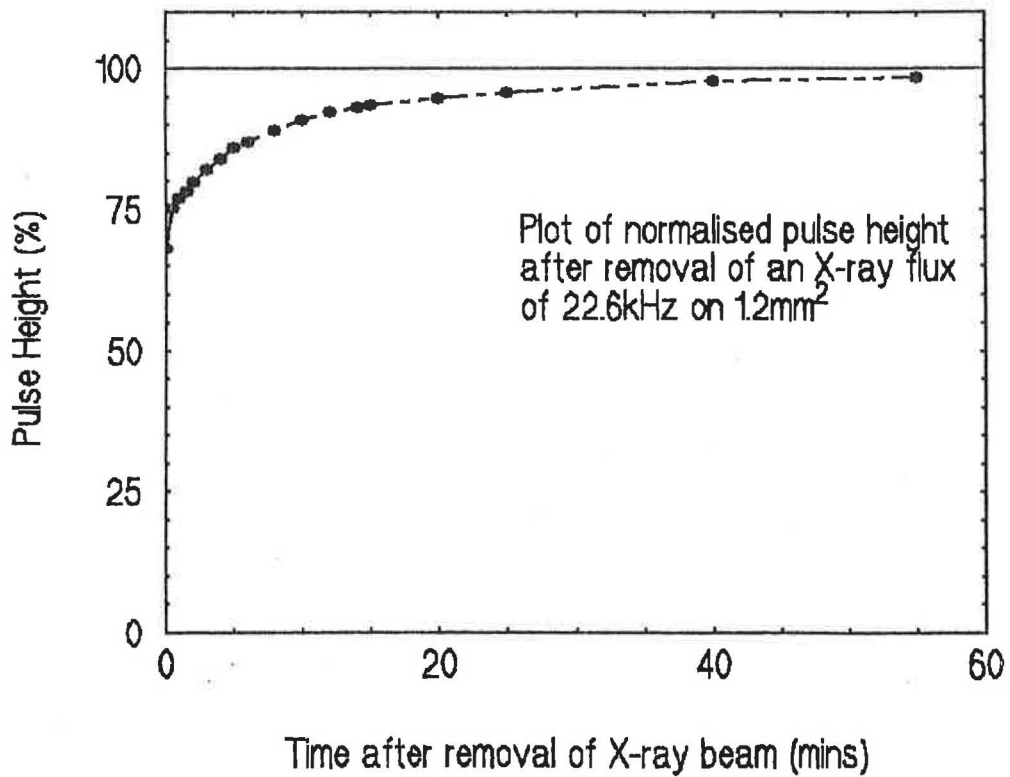


FIGURE 9

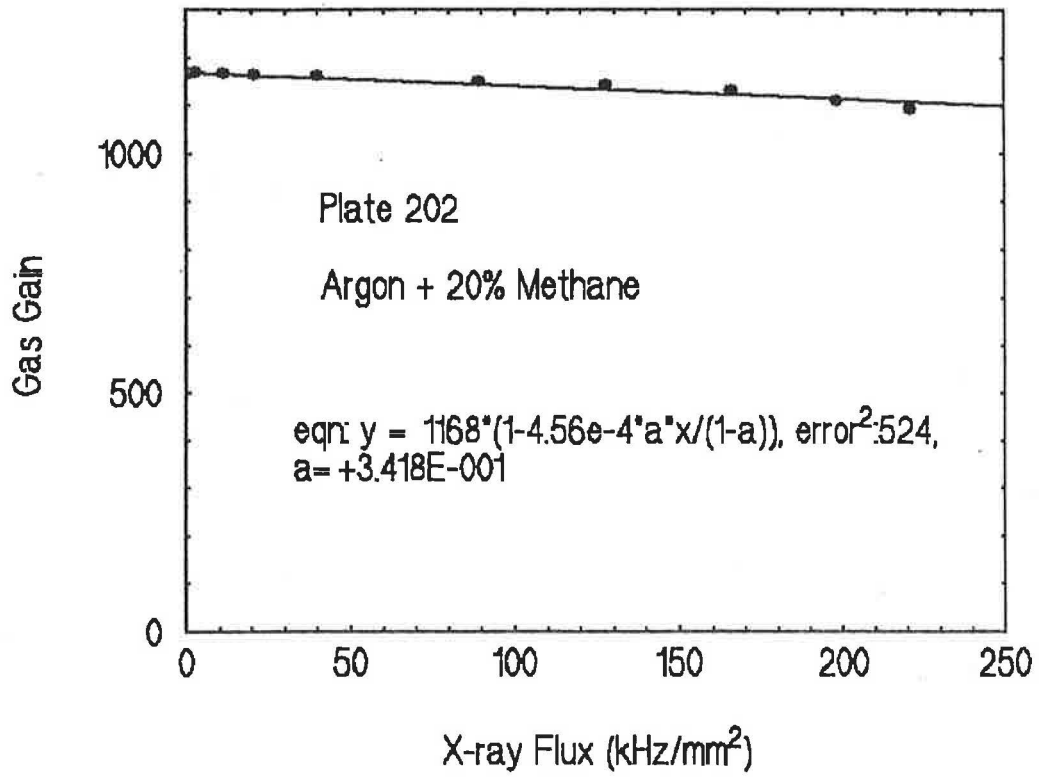
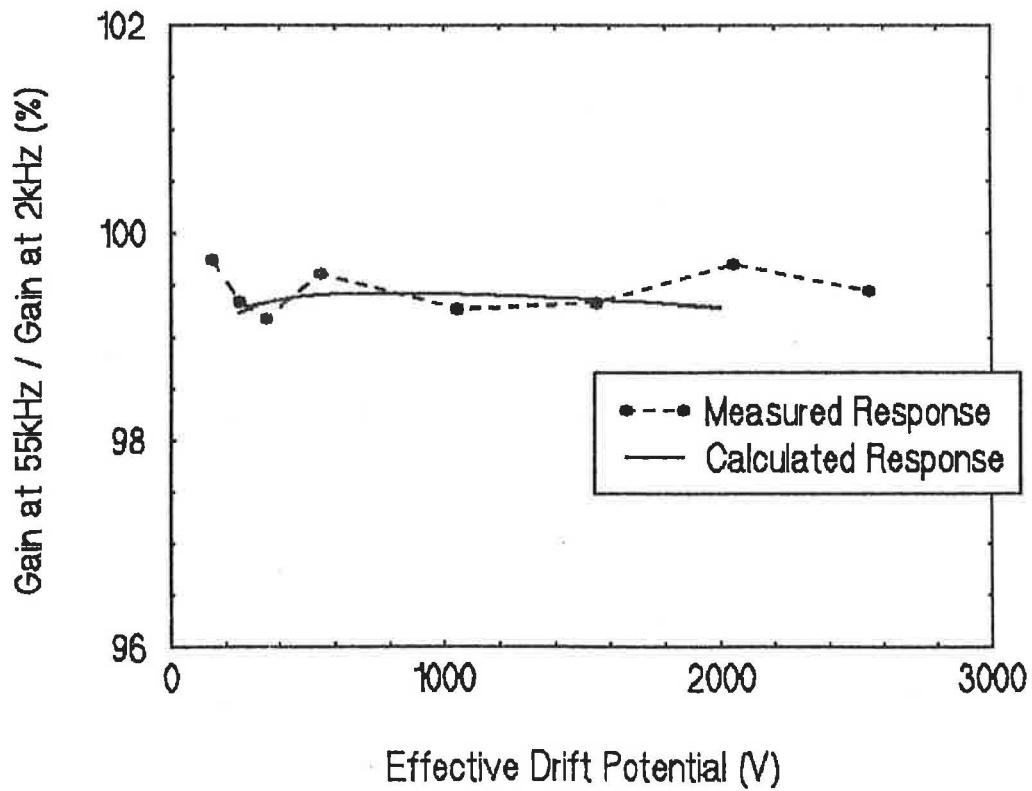


FIGURE 10



the 1990s, the number of people in the UK who are aged 65 and over has increased from 10.5 million to 13.5 million, and the number of people aged 75 and over has increased from 4.5 million to 6.5 million (Office for National Statistics 2000).

There is a growing awareness of the need to address the needs of older people, and the need to ensure that the health care system is able to meet the needs of older people. The Department of Health (2000) has set out a strategy for the health care system to meet the needs of older people, and the Health Service Research Unit (2000) has set out a research agenda for the health care system to meet the needs of older people.

The Health Service Research Unit (2000) has identified a number of key areas for research, and the Department of Health (2000) has identified a number of key areas for research. The Health Service Research Unit (2000) has identified a number of key areas for research, and the Department of Health (2000) has identified a number of key areas for research.

The Health Service Research Unit (2000) has identified a number of key areas for research, and the Department of Health (2000) has identified a number of key areas for research. The Health Service Research Unit (2000) has identified a number of key areas for research, and the Department of Health (2000) has identified a number of key areas for research.

The Health Service Research Unit (2000) has identified a number of key areas for research, and the Department of Health (2000) has identified a number of key areas for research. The Health Service Research Unit (2000) has identified a number of key areas for research, and the Department of Health (2000) has identified a number of key areas for research.

The Health Service Research Unit (2000) has identified a number of key areas for research, and the Department of Health (2000) has identified a number of key areas for research. The Health Service Research Unit (2000) has identified a number of key areas for research, and the Department of Health (2000) has identified a number of key areas for research.

The Health Service Research Unit (2000) has identified a number of key areas for research, and the Department of Health (2000) has identified a number of key areas for research. The Health Service Research Unit (2000) has identified a number of key areas for research, and the Department of Health (2000) has identified a number of key areas for research.

The Health Service Research Unit (2000) has identified a number of key areas for research, and the Department of Health (2000) has identified a number of key areas for research. The Health Service Research Unit (2000) has identified a number of key areas for research, and the Department of Health (2000) has identified a number of key areas for research.